Human Molecular Genetics, 2010, Vol. 19, No. 20 **3959–3969**
doi:10.1093/hmg/ddq311
Advance Access published on July 21, 2010

Genetic ablation of *Dicer* in adult forebrain neurons results in abnormal tau hyperphosphorylation and neurodegeneration

Sébastien S. Hébert[1,2,3,*,†], Aikaterini S. Papadopoulou[3,4], Pascal Smith[1,2], Marie-Christine Galas[6,7], Emmanuel Planel[1,2], Asli N. Silahtaroglu[5], Nicolas Sergeant[6,7], Luc Buée[6,7] and Bart De Strooper[3,4,*,†]

[1]Centre de Recherche du CHUQ (CHUL), Axe Neurosciences, Québec, Canada, [2]Département de Psychiatrie et de Neurosciences, Université Laval, Faculté de Médecine, Québec, Canada, [3]Department of Molecular and Developmental Genetics, VIB, Leuven, Belgium, [4]Center for Human Genetics, K.U. Leuven and [5]Wilhelm Johannsen Centre for Functional Genome Research, Department of Cellular and Molecular Medicine, University of Copenhagen, Copenhagen N, Denmark, [6]Faculté de Médecine, Jean-Pierre Aubert Research Centre, Université Lille-Nord de France, UDSL, Lille, France and [7]Inserm, U837, Alzheimer & Tauopathies, Lille, France

Received April 9, 2010; Revised June 25, 2010; Accepted July 19, 2010

Type III RNase Dicer is responsible for the maturation and function of microRNA (miRNA) molecules in the cell. It is now well-documented that Dicer and the fine-tuning of the miRNA gene network are important for neuronal integrity. However, the underlying mechanisms involved in neuronal death, particularly in the adult brain, remain poorly defined. Here we show that the absence of *Dicer* in the adult forebrain is accompanied by a mixed neurodegenerative phenotype. Although neuronal loss is observed in the hippocampus, cellular shrinkage is predominant in the cortex. Interestingly, neuronal degeneration coincides with the hyperphosphorylation of endogenous tau at several epitopes previously associated with neurofibrillary pathology. Transcriptome analysis of enzymes involved in tau phosphorylation identified ERK1 as one of the candidate kinases responsible for this event *in vivo*. We further demonstrate that miRNAs belonging to the miR-15 family are potent regulators of ERK1 expression in mouse neuronal cells and co-expressed with ERK1/2 *in vivo*. Finally, we show that miR-15a is specifically downregulated in Alzheimer's disease brain. In summary, these results support the hypothesis that changes in the miRNA network may contribute to a neurodegenerative phenotype by affecting tau phosphorylation.

INTRODUCTION

Dicer is a type III RNase enzyme responsible for the processing of microRNA (miRNA) precursors into mature (functional) miRNA molecules. The latter comprises a class of highly conserved small (~20 nt) non-coding RNAs that bind the 3′-untranslated region (3′-UTR) of target messenger RNAs (mRNAs) and regulate gene expression at the post-transcriptional level (1). This results in translational repression or degradation of target mRNAs. Individual or families of miRNAs can target up to several hundred mRNAs, thus controlling complex gene expression pathways and biological systems (2). It has been documented that miRNA family members may have independent and/or overlapping functions *in vivo* (3).

It is nowadays well-established that the fine-tuning of the miRNA gene network is important for the integrity of neuronal populations (4–8). In spite of this, the phenotypes obtained using distinct conditional *Dicer* knockouts in the brain are quite variable, probably reflecting the different aspects of

*To whom correspondence should be addressed. Tel: +1 4186564141 ext. 49233; Fax: +1 4186542753; Email: sebastien.hebert@crchul.ulaval.ca (S.S.H.); Tel: +32 16346227; Fax: +32 16347181; Email: bart.destrooper@cme.vib-kuleuven.be (B.S.).
†The authors wish it to be known that, in their opinion, the first and last authors should be regarded as joint Corresponding Authors.

neurodegeneration in which miRNAs are involved. Using α-CamKII-*Cre* transgenic (Tg) mice that express *Cre* from embryonic day E15.5, Davis *et al*. (6) observed abundant neuronal apoptosis (activated caspase-3 and TUNEL-positive stainings) in the absence of Dicer at early [postnatal day 0 (P0)] but not late (P15) developmental stages. It is worthy of note that these mice did not survive past 21 days of age. In line with this, it has been shown that the removal of *Dicer* at later stages of brain development could contribute to abnormal phenotypes (e.g. increased spine length) but not necessarily neuronal loss (9). The fact that neuronal atrophy but no obvious signs of cell death is observed in *Dicer*-deficient mature striatal neurons is also consistent with this hypothesis (7). It should be mentioned, however, that conditional knockout of *Dicer* in adult Purkinje cells results in a neurodegenerative phenotype accompanied by a limited number of apoptotic (TUNEL-positive) neurons (4).

Hyper- and abnormally phosphorylated forms of the microtubule-associated protein tau characterize neurofibrillary tangles (NFTs) and are observed in more than 20 neurodegenerative disorders including Alzheimer's disease (AD) (10–12). Under physiological conditions, tau promotes the assembly and maintenance of microtubules in neurons and its biological activity is regulated by phosphorylation. It is generally thought that disruption of the normal phosphorylation state of tau plays a key role in the development of NFTs and is intrinsically linked to tau pathology and cell death.

Recent evidence points to a role for miRNA-regulated pathways in modulating tau metabolism and toxicity. Indeed, Bilen *et al*. (13) showed a striking enhancement of tau-mediated toxicity in *Drosophila* cells when miRNA maturation was suppressed. More recently, miR-128 was shown to modulate BAG2 expression in cultured cells, a cochaperone potentially involved in tau degradation and aggregation (14). In thisstudy, we tested the hypothesis that loss of miRNA function could trigger neurodegeneration through mechanisms implicating tau hyperphosphorylation, as seen during neurofibrillary degeneration.

RESULTS

Generation and characterization of mice lacking miRNAs in the adult forebrain

In order to investigate the role of neuronal miRNAs in the adult forebrain, we generated α-CamKII-*Cre* conditional *Dicer* knockout (cKO) mice. The CamKII-Cre transgenic mouse used in this study expresses Cre recombinase mainly in excitatory neurons of the forebrain from approximately P18, with maximal recombination of *loxP*-flanked alleles at 6 weeks (15). Loss of *Dicer* therefore is mainly restricted to the adult cortex and hippocampus.

We first evaluated the biological effects of *Dicer* loss in our mouse model. Starting at ∼9 weeks of age, the *Dicer* mutant animals displayed signs of hypoactivity, had decreased social interaction and were less sensitive to external (e.g. touch) stimuli when compared with littermate controls. At 11 weeks of age, 60% ($n = 16$) of *Dicer* cKO animals had died (Fig. 1A). Consistent with the observations of Davis *et al*. (6), a subset (6 of 16) of *Dicer* cKO mice showed progressive signs of ataxia and/or defects in rear limb movement (data not shown). Four out of 16 mutant *Dicer* mice developed severe tail and/or neck lesions, presumably due to excessive and injurious self-grooming. None of the *Dicer* cKO animals survived past 14 weeks of age (Fig. 1A). On the other hand, control mice ($n \geq 50$) displayed no phenotypic or behavioral abnormalities and survived to adulthood.

To confirm the loss of functional Dicer, miRNA levels were measured by quantitative real-time PCR (qRT-PCR). A significant reduction in brain miRNAs miR-29a, miR-9, miR-134, miR-107 and miR-124 was observed in the cortex of 9-week-old *Dicer* cKO mice when compared with littermate controls (Supplementary Material, Fig. S1A). The changes in miRNA expression are likely underestimated as these samples are composed of a heterogeneous mixture of brain cells (e.g. glia and other neuronal types) and it is not expected that *Cre* is expressed in all the cells.

Neurodegeneration and inflammation in Dicer cKO adult forebrain and hippocampus

At ∼9–10 weeks of age, a considerable (∼25%) reduction in total brain weight was seen in the *Dicer* cKO compared with littermate control mice (Supplementary Material, Fig. S1B). Complete morphological analysis of the brains of *Dicer* cKO mice showed a decrease in size of the cortex, hippocampus (Fig. 1B) and, to a lesser degree, cerebellum. The smaller size of the cerebellum might be the consequence of some residual *Cre* activity in this brain region (6). In the hippocampus of the mutant mice, abundant neuronal loss, particularly in the CA3/4 areas, was evident as shown by stainings with cresyl violet (Fig. 1C) and the neuronal marker NeuN (Supplementary Material, Fig. S1C). In the cortex, a different image was observed. NeuN stainings showed clear signs of cytoplasmic atrophy, but no obvious neuronal loss (Fig. 1D; controls = 100% versus *Dicer* cKO = 107 ± 17%, $n = 3$ from each group). The reduction in size, but not in the total cell number, is in line with the decrease in the 48-kDa cytoplasmic (versus 46-kDa nuclear) NeuN variant (16) and the equal amounts of neuronal marker MAP2 (Fig. 1E). No indications of apoptosis using activated caspase-3 as well as fragmented DNA [using 4′,6-diamidino-2-phenylindole (DAPI)] stainings were observed in the different *Dicer* cKO brain regions (Supplementary Material, Fig. S2).

An increase in the microglial activation marker Iba1 was observed in the hippocampus of 9-week-old *Dicer* cKO compared with littermate control mice (Fig. 1Fa–d). We could only consistently detect Iba1-positive stainings in the cortex of 12.5-week-old mutants (Fig. 1Fe and f). Similarly, at 12.5 weeks (but not at 9 weeks), an increase in glial fibrillary acidic protein (GFAP)-positive astrocytes was observed in the cortex and hippocampus of mutant *Dicer* animals (Fig. 1Ga–d). Taken together, these results show that the absence of functional Dicer in the adult forebrain is accompanied by progressive neuronal degeneration as well as increased inflammation and gliosis.

Tau hyperphosphorylation in the absence of Dicer

To analyze the tau phosphorylation levels in the cortex of 9-week-old *Dicer* cKO mice, endogenous tau proteins were

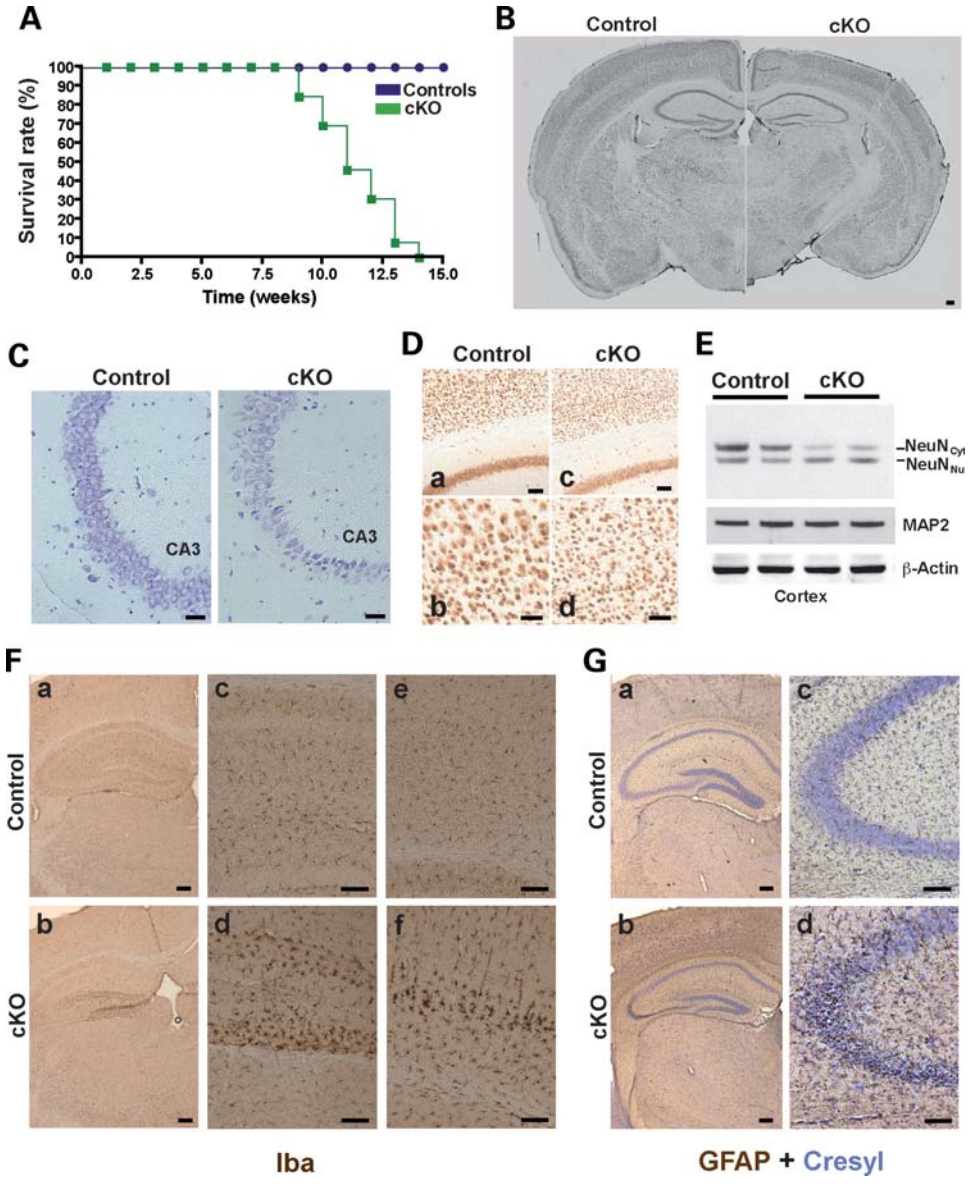

Figure 1. Early death and neurodegeneration in adult α-CamKII/Dicer cKO mice. (**A**) The Kaplan–Meier plot of survival demonstrates that 60% of CamKII-*Cre*/+;*Dicer*$^{flox/flox}$ ($n = 16$; green square) animals die by 11 weeks of age. No animals survive after 14 weeks of age. The control animals CamKII-*Cre*/+;*Dicer*$^{flox/+}$ and +/+;*Dicer*$^{flox/flox}$ survive into adulthood ($n \geq 50$, blue circle). (**B**) Complete morphological analysis of 9-week-old control and *Dicer* cKO brains. Cells were stained with the neuronal marker NeuN. A representative image (montage) is shown. Note the reduction in size of the cortex and hippocampus (more particularly the CA3/4 regions) in the *Dicer* cKO compared with control. Scale bar = 150 μm. (**C**) Representative ($n = 2$ from each group) crystal violet stainings demonstrating massive neuronal loss in the hippocampus CA3 region of 9-week-old *Dicer* cKO mice. Scale bar = 15 μm. (**D**) Representative ($n = 3$ from each group) immunohistochemistry of NeuN in the cortex of 9-week-old control (a, magnified in b) compared with *Dicer* cKO (c, magnified in d) mice. Scale bars = 40 μm (b and d) and 20 μm (a and c). (**E**) Western blot analysis of NeuN and MAP2 in cortex samples of 9-week-old control and *Dicer* cKO mice. NeuN Cyt (cytoplasmic) variant is reduced, whereas NeuN Nu (nuclear) remains unchanged in the mutant mice. Two mouse samples from each group are shown. For quantitative analysis, the ratios of NeuN cytoplasmic versus nuclear are indicated for each sample. β-Actin was used as internal loading control. (**F**) Representative ($n = 3$) immunohistochemical studies revealed the accumulation of Iba1 in 9-week-old *Dicer* cKO (b, magnified in d) compared with control (a, magnified in c) hippocampus. Iba1-positive stainings were equally present in the cortex of 12.5-week-old *Dicer* cKO mice (f) when compared with controls (e). Scale bars = 75 μm (a and b), and 80 μm (c and d–f). (**G**) GFAP immunoreactivity is increased in the hippocampus (b and d) and cortex (b) of *Dicer* cKO compared with control (a and c) animals at 12.5 weeks. Crystal violet stainings of cells are shown. Scale bars = 75 μm (a and b) and 80 μm (c and d).

resolved by two-dimensional (2D) electrophoresis and labeled with antiserum directed against total tau. A shift of all major murine tau isovariants to the acidic side was observed in the *Dicer* cKO mice when compared with littermate controls (Fig. 2A). Further characterization of tau phosphorylation was performed using a panel of phospho-tau antibodies (Fig. 2B). These eastern blotting experiments confirmed that endogenous tau in the *Dicer* cKO brains is hyperphosphorylated at several sites, comprising epitope AT8 (Ser202/Thr205), AT180 (Thr231), AT270 (Thr181), AD2/PHF-1

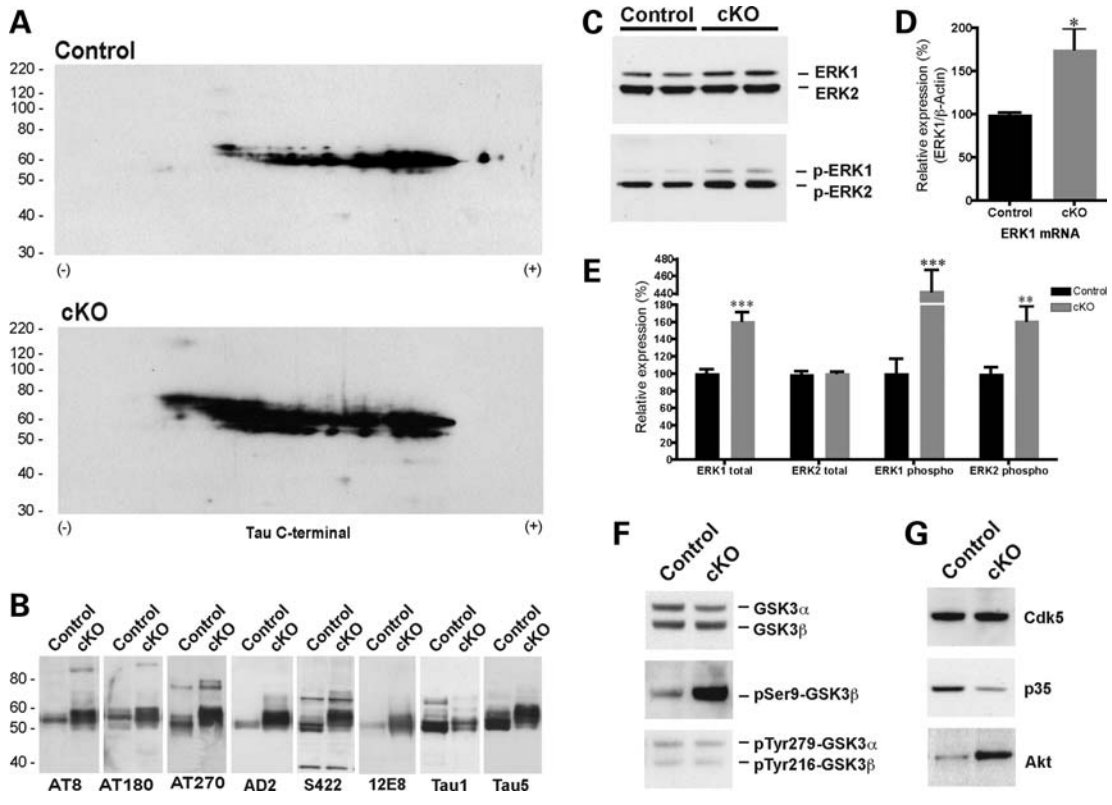

Figure 2. Pathological hyperphosphorylation of endogenous tau in the absence of Dicer. (**A**) 2D gel analysis of cortex samples from control and *Dicer* cKO 9-week-old mice. Note the shift in weight of tau isovariants (10) in the mutant animal. Blots were probed using a total tau Cterm1902 antibody. (**B**) Western blot analysis of endogenous tau using a variety of anti-phospho antibodies. Note the increase in tau molecular weight in the mutant samples. (**C** and **E**) A specific increase in ERK1 (compared with ERK2) protein and phosphorylation levels in the conditional *Dicer* KO mice. A weak increase in ERK2 phosphorylation is observed as well. Representative results ($n \geq 5$ per group) are also shown. Equal amount of proteins were loaded in each lane. (**D**) qRT-PCR of ERK1 mRNA levels (in percentage) of control ($n = 3$) and *Dicer* cKO ($n = 4$) mice. β-Actin was used as qRT-PCR normalization control. The relative expression (in percentage) of ERK1 mRNA was calculated using the relative quantification method (using the average of controls as 100%). (**F**) An increase in GSK-3β Ser9 phosphorylation in the *Dicer* cKO animals. (**G**) Changes in the Cdk5/Akt pathways in the mutant *Dicer* mice compared with controls. Statistical significance was determined by a Student's paired *t*-test, where $^{*}P < 0.05$, $^{**}P < 0.01$ and $^{***}P < 0.001$.

(Ser396/Ser404), 12E8 (Ser262/Ser356) and the 'pathological' S422 (Ser422) (17). The shift in the molecular weight of tau is consistent with its hyperphosphorylation state. Tau1 (dephosphorylated amino acid 189–207) was decreased in the *Dicer* cKO mice, in line with the hyperphosphorylation of tau at this epitope. The global amount of tau protein was not altered as controlled using the Tau5 (amino acid 210–241) antibody. Moreover, qRT-PCR showed that total tau mRNA was also unchanged between the *Dicer* KO and control groups (Supplementary Material, Fig. S3A). Notably, similar to the cortex, increases in tau hyperphosphorylation were observed in the hippocampus of *Dicer* mutants (Supplementary Material, Fig. S3B). In addition, no change in tau phosphorylation was evident in younger (3–7 weeks old) *Dicer* cKO mice (Supplementary Material, Fig. S3C). Overall, these results show a site-specific and time-dependent hyperphosphorylation of endogenous tau *in vivo* in the absence of functional Dicer in the adult brain.

Finally, we evaluated the effects of Dicer loss on tau phosphorylation in neuronal cell cultures. To this end, we performed transient knockdown experiments in Neuro2a cells using short hairpin RNAs directed against *Dicer* mRNA. Seventy-two hours after transfection, we observed a significant increase in endogenous tau phosphorylation (Supplementary Material, Fig. S3D and E) upon Dicer knockdown. We confirmed the downregulation of Dicer in these experimental conditions by western blot (Supplementary Material, Fig. S3F) and qRT-PCR (data not shown).

ERK1 levels are increased in Dicer cKO brains

As it is unclear how Dicer deficiency can lead to tau hyperphosphorylation, we hypothesized that miRNA-regulated pathways could affect the kinases or phosphatases involved in tau phosphorylation. We, therefore, screened for potential candidates using Affymetrix gene expression arrays. We focused on upregulated kinases or downregulated phosphatases involved in tau phosphorylation and set a ± 1.25-fold change in expression with $P < 0.01$ as cutoff values. Among several candidate enzymes (18), these screens identified mitogen-activated protein kinase 3 (MAPK3/ERK1) to be specifically upregulated in the *Dicer* cKO mice (Supplementary Material, Tables S1 and S2). Although protein phosphatase 2C was significantly downregulated in the *Dicer* cKO mice, this enzyme was previously shown to be only weakly involved in direct tau dephosphorylation (19). We therefore

focused our work on ERK1. To validate the microarray data, we performed qRT-PCR and western blot analyses. These experiments showed an increase in ERK1 at the mRNA, protein and phosphorylation levels in the *Dicer* mutant mice (Fig. 2C–E). To a lesser extent, a significant increase in ERK2 phosphorylation (but not protein levels) was also observed.

Other kinases considered to be *in vivo* responsible for the regulation of tau phosphorylation include GSK-3β and Cdk5 (20,21). GSK-3β activity is regulated negatively by the phosphorylation of serine 9 (Ser9) and positively by phosphorylation of tyrosine 216 (Tyr216). Western blot analysis of equal amounts of protein showed a drastic increase in GSK-3β Ser9 phosphorylation in the cortex of *Dicer* cKO mice when compared with littermate controls (Fig. 2F). In contrast, no changes at the GSK-3β Tyr216 site as well as in GSK-3β total protein levels were observed in the mutant *Dicer* mice.

In the brain, Cdk5 is activated by its interaction with the neuron-specific molecule, p35, or the p35-cleaved product p25. Although Cdk5 total protein levels remained unchanged, a reduction in p35 levels without p25 formation was observed in the mutants (Fig. 2G). The PKB/Akt survival pathway is known to be involved in GSK-3β Ser9 phosphorylation. A marked increase in Akt protein levels was detected in the *Dicer* cKO brains (Fig. 2G), which could explain the observed effects on GSK-3β Ser9. Of notice, Akt and p35 mRNAs were also upregulated and downregulated, respectively, in our microarray analysis (Supplementary Material, Table S1 and data not shown). Taken together, these results suggest that the GSK-3β/cdk5 pathway is downregulated and therefore not mainly involved in tau hyperphosphorylation in the absence of Dicer.

Finally, there were no significant changes at the protein and activity levels of other mitogen-activated protein kinase family members, namely JNK1 and 2, as well as several major tau phosphatases including PP1, PP2B, PP2AA and PP2AC (Supplementary Material, Fig. S4 and data not shown). Overall, we identify ERK1 (and perhaps ERK2) as a candidate effector of tau hyperphosphorylation *in vivo* in the conditional *Dicer* KO mice.

miR-15 family members regulate ERK1 expression

The increase in ERK1 protein (and mRNA) levels in the *Dicer* cKO mice prompted us to investigate whether dysregulation of particular miRNAs could be involved in the regulation of ERK1 expression. We used common prediction programs (*TargetScan* and *miRANDA*) to search for potential miRNA target sites on the 3′-UTR of ERK1 mRNAs. These screens identified conserved miRNA seed sequences for the miR-15/16/195/322/497 and miR-1/206 families (Supplementary Material, Fig. S5A and B). We focused our work on the miR-15 family, as miR-1/206 family members are mainly expressed in muscle cells and not in the brain (22). Compared with control brains, miR-15a, miR-195, miR-16 and miR-497 expression levels were significantly reduced in 9-week-old *Dicer* cKO mice, whereas no significant change was observed for miR-15b and miR-322 in these samples (Supplementary Material, Fig. S5C).

We further evaluated the possibility that ERK1 expression could be regulated by miRNA expression. miRNA precursors (pre-miRs) for miR-15a, miR-16, miR-195 and miR-497 were transfected in Neuro2a cells causing a significant (∼55–85%) reduction in endogenous ERK1 protein and phosphorylation levels (Fig. 3A and B). As negative control, we used a scrambled miRNA sequence. We also verified that blocking endogenous miR-16, which is highly expressed in neuroblastoma Neuro2a cells (Supplementary Material, Fig. S5D), results in a ∼50 and ∼250% increase in ERK1 protein and phosphorylation levels, respectively (Fig. 3C). Here, a scrambled miRNA inhibitor was used as a negative control. Of note, a small but significant increase in ERK2 phosphorylation was equally observed in anti-miR-16-treated cells. In these experimental conditions, a significant (∼50–90%) reduction in endogenous miR-16, miR-15a, miR-195 and miR-497 was observed (Supplementary Material, Fig. S5E), likely because of the similarities of these miRNA family members and cross-reactivity of the antisense locked nucleic acid (LNA) probes. These loss of function experiments in cells demonstrate at the endogenous level of expression that miR-16 and related family members are involved in the fine-tuning of ERK1 expression (including ERK1/2 phosphorylation).

To test whether the candidate miRNAs target directly the ERK1 mRNA, we performed luciferase assays using the isolated ERK1 3′-UTR. We found that pre-miR-15a, miR-16, miR-195 and miR-497 affected indeed significantly (∼70–80%) luciferase expression (Fig. 3D and E). In contrast, a scrambled miRNA sequence showed no effect. We mutated the two potential miR-15 family target sites of the mouse ERK1 3′-UTR (Fig. 3D, see also Targetscan.org) which abolished partially or completely the suppressing effects of miR-15 family members (Fig. 3E). Next, we could demonstrate that ERK1 mRNA levels were reduced in pre-miR-15a and 195-treated Neuro2a cells, indicating that these miRNAs promote ERK1 mRNA decay (Fig. 3F). These results are consistent with the hypothesis that miRNAs modulate ERK1 mRNA stability in the mouse brain (Fig. 2D). Finally, and consistent with previous findings (23,24), we could show that ERK1/2 and miR-195 are expressed in the same cells in the brain (Fig. 3G).

The miR-15/ERK pathway can regulate tau phosphorylation

We next sought independent validation for the role of ERK1/2 in the regulation of tau phosphorylation. For this, we used the inhibitor U0126, which inhibits kinases MEK1/2, ERK1/2 activating kinases. Treatment of Neuro2a cells with U0126 caused a marked decrease in endogenous tau AT8 immunoreactivity, whereas Tau1 reactivity was increased (Fig. 4A). Total tau was not significantly changed in these conditions. Thus, endogenous ERK1/2 activity regulates tau phosphorylation, at least in these cells. We also evaluated the role of the identified miRNAs in regulating tau phosphorylation in primary neurons. Ectopic expression of pre-miR-16 in primary cortical rat neurons induced a marked upregulation of Tau1 stainings (Fig. 4B). Similar results were obtained using pre-miR-15a (data not shown). Notably, no change in total tau was observed in these conditions. We also measured

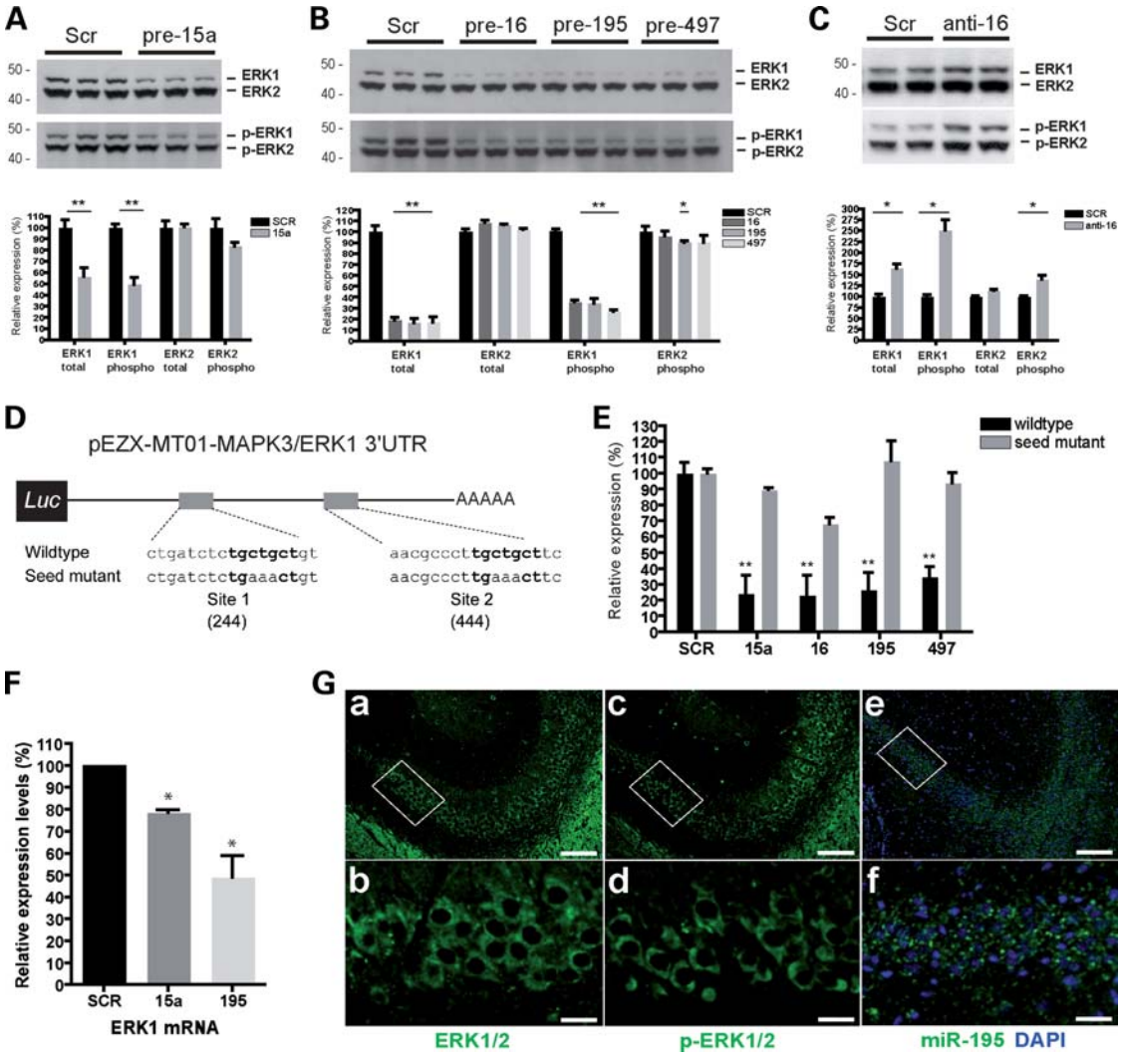

Figure 3. Regulation of ERK1 by miR-15 family members. (**A** and **B**) Western blot analysis of endogenous total and phospho-ERK1 and ERK2 in Neuro2a cells treated with 100 nM of indicated pre-miRs. A scrambled oligonucleotide sequence (Scr) was used as control. Note that no change in ERK1 expression was observed in untransfected versus Scr-transfected cells (data not shown). Quantifications (in percentage) are shown as 100% using the average Scr-treated cells. Equal amount of proteins were loaded in each lane. Triplicate samples are shown. (**C**) Western blot analysis of endogenous total and phospho-ERK1 and ERK2 in Neuro2a cells treated with 100 nM of LNA-modified anti-miR-16. A scrambled LNA oligonucleotide sequence (Scr) was used as control. Quantifications (in percentage) are shown as 100% using the average Scr-treated cells. Note the significant increase in ERK2 phosphorylation levels in the anti-miR-16-treated cells. Equal amount of proteins were loaded in each lane. (**D**) Schematic representation (not to scale) of the ERK1 3′-UTR luciferase construct used in this study. *Luc*, luciferase gene. The sequence and the 'top score' putative binding sites for miR-15 family members are shown. The miRNA seed sequences are in bold. In the ERK1 3′-UTR mutant constructs (site 1 or site 2), the binding sites for miR's are mutated as indicated. (**E**) ERK1 3′-UTR wild-type or double-seed mutant luciferase constructs were co-transfected into Neuro2a cells with the indicated pre-miRNA oligonucleotides at a final concentration of 100 nM. Quantifications (in percentage) are shown as 100% using the average Scr-treated cells. (**F**) qRT-PCR of ERK1 mRNA levels (in percentage) of Neuro2a cells treated with 100 nM of pre-miR-15a, pre-miR-195 or a control scrambled sequence. The average value of two independent experiments (in duplicate) is shown. β-Actin was used as qRT-PCR normalization control. Statistical significance was determined where indicated by a Student's paired *t*-test; $^{*}P < 0.05$ and $^{**}P < 0.01$. (**G**) Immunohistochemical studies indicating total ERK1/2 (a) and phospho-ERK1/2 (c) expression (in green) in the hippocampus of adult wild-type mice. Note the cytoplasmic localization of ERK1/2. Overlapping expression patterns of miR-195 (in green) in the hippocampus as observed by *in situ* hybridization (e). Note the puncta-like localization in the cytoplasm. Here, the cell nucleus is revealed using DAPI stainings. Magnifications of CA1/2 (b, d and f) areas are shown. Scale bars = 40 μm (a, c and e) and 15 μm (b, d and f).

endogenous tau phosphorylation in miRNA loss-of-function paradigms. Inhibition of endogenous miR-16 in primary neurons resulted in a significant increase in tau AT8 immunoreactivity (Fig. 4C). We confirmed these changes by western blot (Fig. 4D). Taken together, these findings indicate that specific miRNAs can regulate tau phosphorylation under physiological conditions.

Finally, we explored the hypothesis that loss of miRNA function could contribute to tau pathology in humans. To this end, we performed miRNA qRT-PCR from control and sporadic AD cases. Previous studies have shown that miR-16 is stably expressed in human tissues, including AD brain (25–27). Using this miRNA as internal control, we observed a significant decrease in miR-15a expression levels

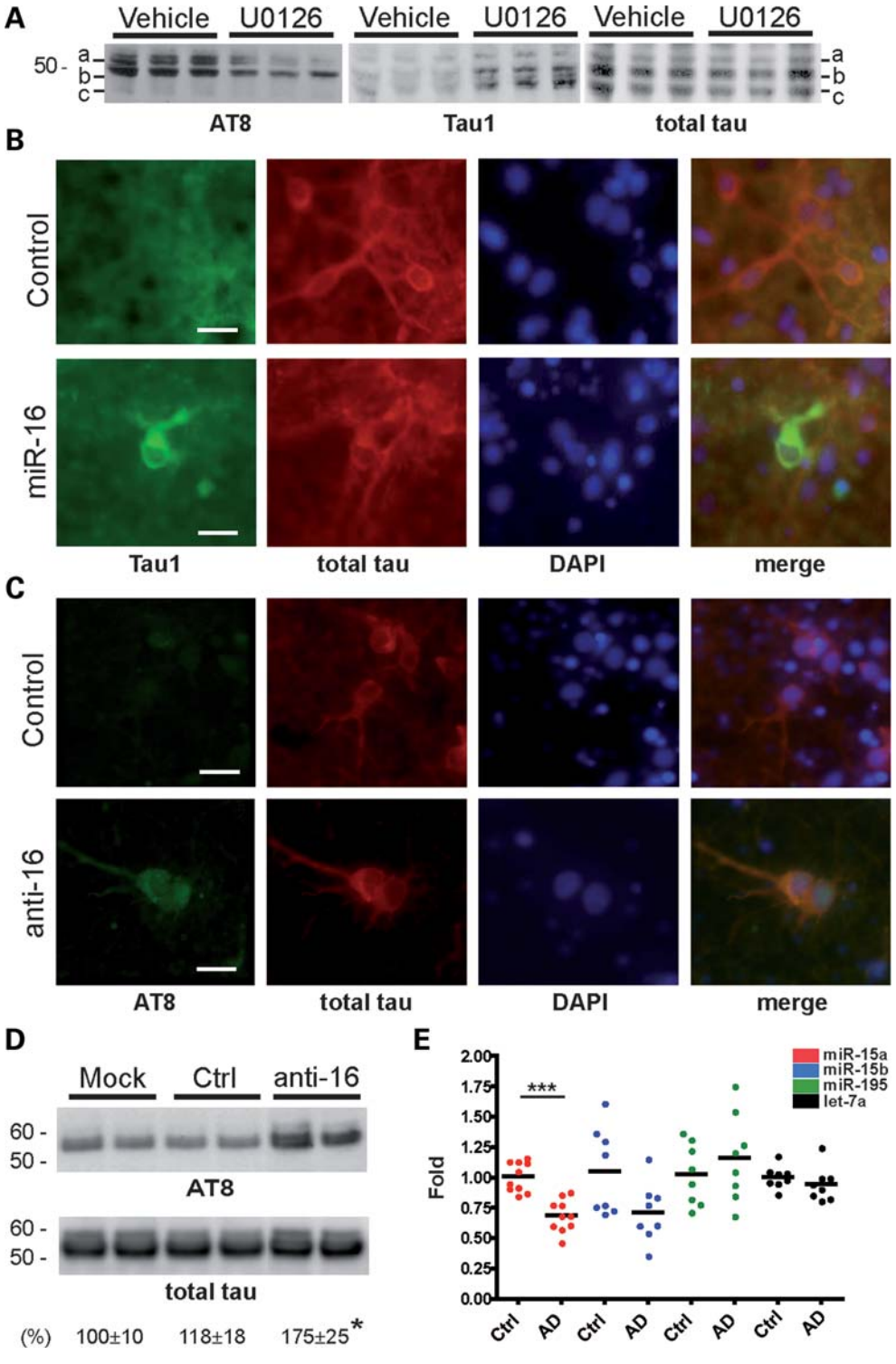

Figure 4. ERK1/2 and miRNA regulation of tau phosphorylation. (**A**) Western blot analysis of endogenous tau (AT8, Tau1 and total Tau) in the presence of 10 nM U0126 or vehicle (DMSO). Note the isoform-dependent effects (depicted as 'a', 'b' or 'c') on tau phosphorylation (AT8) and dephosphorylation (Tau1) in Neuro2a cells. Triplicate samples are shown. (**B**) Immunohistochemical studies of endogenous Tau1 (in green) and total tau (in red) in DIV9 rat primary cortical neurons treated with 200 nM of pre-miR-16 or control (pre-miR-1). (**C**) Immunohistochemistry of endogenous tau AT8 (in green) and total tau (in red) in neurons treated with 200 nM of anti-miR-16 or control (anti-miR-1). In both cases, the nuclei were stained using DAPI. Scale bar = 10 μm (all panels). (**D**) Anti-miR-16-treated (200 nM) primary neurons were processed for immunoblot analysis using tau AT8 and total tau (Cterm) antibodies. Here, non-transfected (mock) or control (anti-miR-1) mice were used as negative controls. Note the significant (~75%) increase in tau AT8/total tau immunoreactivity in the antisense-treated cells ($n = 3$ from each group). (**E**) qRT-PCR of mature miR-15a, miR-15b, miR-195 and let-7a in controls ($n = 8$–10) and AD patients ($n = 8$). Relative expression is shown as percentage using the mean of the controls group as reference. The graph mean is shown. In all experiments, ubiquitously expressed miR-16 was used as normalization control. Every data point reflects the mean of three independent RT reactions. Statistical significance was determined by a Student's paired *t*-test; $^{*}P < 0.05$ and $^{***}P < 0.001$.

in AD brain when compared with healthy controls (Fig. 4C). There was no significant change in the expression of other miR-15 family members, including miR-15b and miR-195. We used as additional control the ubiquitously expressed let-7a, which is not affected in both groups. These results, together with previously published miRNA microarray data (27,28), strongly suggest that specific miR-15 family members, such as miR-15a, are affected in compromised brain displaying tau hyperphosphorylation.

DISCUSSION

We show here that loss of *Dicer* in the adult forebrain impairs the expression of several miRNAs ultimately leading to pathological hyperphosphorylation of tau, the latter being observed in various neurodegenerative disorders. Abnormal tau phosphorylation coincides with neurodegeneration and behavioral abnormalities. We further identify ERK1 (and to a lesser extent ERK2) to be increased in the *Dicer* knockout mice and provide *in vitro* evidence that ERK1 could be one candidate effector of tau hyperphosphorylation. We show that miR-15 family members, whose levels are reduced in the *Dicer*-deficient animals, can regulate ERK1 expression and phosphorylation as well as tau phosphorylation in cultured mouse neurons. Finally, we could show that miR-15a is downregulated in AD brain. Overall, these results provide strong evidence that misregulation of the miR-15 network may contribute to tau pathology in compromised brain. The biological relevance of our observations is further corroborated by *in situ* hybridization and immunohistochemistry experiments showing co-expression of miR-195 and ERK1/2 in brain. Obviously, we cannot exclude the contribution of other miRNAs or enzymes in the effects we observed in the *Dicer* KO mice at this stage of investigation.

In contrast to previous studies (4–7), ablation of *Dicer* function in mature excitatory neurons results in a mixed degenerative phenotype, characterized by neuronal loss mainly in the CA3/4 areas of the hippocampus and neuronal atrophy which seems predominant in the cortex, which was associated with gliosis. The most salient feature of our model is, however, the dramatic increase in tau phosphorylation, which adds an important component to the neurodegenerative phenotypes observed in various *Dicer* knockout models. It is noteworthy to mention that abnormal tau phosphorylation and aggregation can cause caspase-3-independent neuronal death *in vivo*. In addition, sustained activation of ERK can result in neuronal death (29,30). Whereas GFAP and Iba1 stainings were negative in the cortex of 9-week-old mice, we cannot exclude the role of inflammation in mediating tau hyperphosphorylation and neurodegeneration. This possibility warrants further investigation.

It is likely that cell-type or tissue-specific changes in miRNA expression patterns or survival pathways could account for the observed distinctive neurodegenerative phenotypes in different *Dicer* KO models. We believe that in our model the tau phosphorylation which occurred concomitantly in the different affected brain regions, might explain, at least in part, the observed morphological and behavioral phenotypes. For instance, it is possible that abnormal tau phosphorylation has a direct impact on the cytoskeleton causing neurons to 'shrink' in the cortex. In the hippocampus, neurons may be more sensitive to such events resulting in faster neuronal loss. Although toxic accumulation of proteins into autophagic-like vacuoles is another interesting alternative to the cause of neuronal death in the absence of Dicer (4), our preliminary western blot data suggest no changes in autophagic markers LC3-I/II, Beclin1, ATG5-12 and ATG16L1 in the mutant *Dicer* cKO brain (data not shown). On the other hand, our study strongly suggests that ERK1/2 and tau hyperphosphorylation could contribute to neurodegeneration, but further investigation is needed to address the detailed molecular mechanisms involved in *Dicer*-mediated neuronal loss in adult neurons.

It is of interest that total tau protein and mRNA levels remain unchanged in *Dicer*-less brain, which suggests that miRNAs play only a limited role in the direct regulation of tau expression *in vivo*, at least in the neurons and developmental stage we investigated here. We find, however, that ERK1, one of the kinases phosphorylating tau, was increased at the mRNA, protein and phosphorylation levels in the conditional *Dicer* KO mice. The marked elevation in ERK1 phosphorylation (~450%) compared with its protein (~50%) levels may represent a feed-forward autophosphorylation mechanism of ERK1 (31) and maybe ERK2. The hyperphosphorylation of tau at several sites (Thr181, Ser202, Thr205, Thr231, Ser396, Ser404 and Ser422) is fully consistent with a predominant role for ERK1/2 in this pathological process (18). The hyperphosphorylation of endogenous tau at the S422 site is of particular interest because of its direct link to neurofibrillary pathology in AD, and an increase in ERK1/2 phosphorylation is observed in neurons displaying tau pathology in human AD brain (30,32,33). Taken together, these results strengthen the role of ERK1/2 in the pathological phosphorylation of tau *in vivo*. Whether sustained activation of ERK1 (and ERK2) in the brain can completely recapitulate tau pathology and neurodegeneration, remains an interesting possibility, but difficult to explore in our model given its early lethality.

Our results, combined with others, start to provide quite impressive support for the concept that changes in the miRNA network can contribute importantly to several aspects of the neurodegenerative process in AD and other diseases. This is corroborated by several studies that have detected changes in miRNA expression patterns in AD brain (8,27,34–36). Several of those affected miRNAs seem to participate directly in the regulation of expression of disease-related proteins, namely APP (37–39) and BACE1/β-secretase (27,36), both involved in neurotoxic Aβ peptide production. In this study, we provide evidence that also the other limb of the neurodegenerative process in AD, i.e. the progressive abnormal phosphorylation of tau and potentially its accumulation in tangles, could be promoted by loss of specific miRNAs, which regulate the ERK kinase in AD brain.

In conclusion, our findings add to the accumulating evidence that misregulation of miRNA pathways could contribute significantly to neurodegenerative disorders in humans (8,40–42). One can expect a progressive dysregulation of this finely tuned network with aging, which according to these data would set the stage for various neurodegenerative processes.

MATERIALS AND METHODS

Cells, transfections and treatments

Neuro2A cells were cultured in DMEM/F12 medium supplemented with 10% FCS. Subconfluent cells were transfected with 100 nM of pre-miRs (Pre-miR miRNA Precursor Molecules, Ambion) or anti-miRs (LNA-inhibitors, Exiqon) using LipofectAMINE 2000 following the manufacturer's instructions. Forty-eight hours post-transfection, cells were processed for immunoblot analysis. For the MEK1/2 inhibition, Neuro2a cells were treated for 48 h with 10 μM U0126 (Sigma) or vehicle (DMSO) prior to immunoblot analysis.

Rat primary cortical cultures were prepared as described previously (43). Nine days after seeding, the culture media was removed and replaced with 500 μl of fresh neurobasal medium supplemented with B27 and glutamine. Cells were incubated 24 h prior to transfection. Then, 1 μl of LipofectAMINE 2000 was diluted in 50 μl of OptiMEM per well (24 wells plate) and incubated at room temperature for 5 min. Fifty microlitters of OptiMEM were combined with 2.4 μl solution of 50 μM miRNA (final dilution 200 nM). The diluted miRNA and LipofectAMINE were mixed and incubated at room temperature for 20 min. One hundred microlitters of OptiMEM containing the miRNA/LipofectAMINE transfection complexes were added to each well. Tau phosphorylation was evaluated 48 h from the start of transfection.

For the luciferase assays, 100 nMpre-miRs (Ambion) were co-transfected with the full-MAPK3 length mouse 3′-UTR luciferase vector (GeneCopoeia cat# MmiT030696-MT0). Mutagenesis was performed by TopGeneTech (Montreal, Canada) and confirmed by sequencing. Twenty-six to 28 h post-transfection, the measurements were performed using the Dual luciferase reporter assay kit (Promega).

Mice

The generation and characterization of *α-CamKII-Cre* Tg transgenic mice was described previously (15). The *Dicer* floxed mice (*Dicer*$^{flox/flox}$) were generously provided by M. McManus (University of California, CA, USA) (44). To obtain forebrain-specific *Dicer* cKO mice (CamKII-*Cre*/+; *Dicer*$^{flox/flox}$), we crossed floxed *Dicer* (*Dicer*$^{flox/flox}$; *Dicer*$^{flox/flox}$) mice with *CaMKII-Cre* Tg mice. Experimental mice (CamKII-*Cre*/+;*Dicer*$^{flox/flox}$, designated 'cKO') and littermate control mice (CamKII-*Cre*/+;*Dicer*$^{flox/+}$ or +/+; *Dicer*$^{flox/flox}$, designated 'Control') were used. No differences at the behavioral, morphological and biochemical levels were observed among control mice. All mice were bred on a C57BL/6 background.

Antibodies

For a list of antibodies, please refer to Supplementary Material.

Protein extraction and western blot analysis

Cells were rinsed with cold PBS and lysed in buffer: 1% Triton X-100, 50 mM HEPES, pH 7.6, 150 mM NaCl, 1 mM EDTA and complete protease inhibitors (Roche). Protein from mouse brain was extracted using the miRVana PARIS kit (Ambion). Immunoblot analysis was performed as described (45). 2D gel electrophoresis was performed as described previously (46).

RNA extraction and qRT-PCR

Total RNA was extracted from brains and cells using the miRVana PARIS kit (Ambion) according to the manufacturer's instructions. RT-PCR and quantitative PCR procedures were carried out as described (45). Primer sequences to quantify mouse ERK1 are: forward 5′-ATGAAGGCCCGAAACT ACCT-3′, reverse 5′-CCTCTACTGTGATGCGCTTG-3′. For miRNA quantifications, probe-specific TaqMan miRNA assays (Applied Biosystems) were used according to the manufacturer's instructions. Relative expression was calculated by using the comparative C_t method. For mouse quantifications, RNU19 (Applied Biosystems) was used as a normalization control.

Microarray analysis

Microarray details can be found in Supplementary Material.

Immunohistochemistry and *in situ* hybridization

NeuN, Iba-1 and GFAP immunohistochemical as well as cresyl violet stainings were done as described previously (47). ERK1/2 immunohistochemistry was performed as described previously (48). *In situ* hybridization for miR-195 was performed as described previously (23,27). A scrambled miRNA as well as no probe were used as negative controls (data not shown). All assays were done on adult (∼2 months old) mice. For primary neurons, cells were fixed in cold 4% paraformaldehyde and 0.05% glutaraldehyde for 30 min at room temperature. Permeabilization was carried out in 0.2% Triton X-100 in phosphate-buffered saline for 10 min. After a 30 min saturation in 2% bovine serum albumin, immunostainings were carried out using AT8, Tau1 and tau total (Cterm) antibodies. Tau1 and AT8 stainings were revealed with a goat anti-mouse IgG (H + L) antibody coupled to Alexa Fluor488 (Molecular Probes). Total tau staining was revealed with a goat anti-rabbit IgG (H + L) antibody coupled to Alexa Fluor568 (Molecular Probes). DAPI was added to the mounting medium. Slides were analyzed with a Zeiss fluorescence light microscope.

Statistical analyses

ERK1/2 and NeuN densitometric quantifications were performed using the ImageJ software. Statistical significance was determined using a Student's paired *t*-test as indicated in the text. Calculations were made using the GraphPad Prism 4 software. NeuN positive cells (nuclei) were counted from layers IV/V of the mouse cortex (three fields per brain) using the Photoshop CS3 program. Data were normalized as percentage to littermate controls (set as 100%).

SUPPLEMENTARY MATERIAL

Supplementary Material is available at *HMG* online.

ACKNOWLEDGEMENTS

We would like to thank Dr André Delacourte (Lille, France) and the Lille Neurobank for generously providing us with the human brain samples. We also thank Drs Michael T. McManus and Trinna L. Cuellar (University of California, CA, USA), as well as Dr Jie Shen (Brigham and Women's Hospital, USA) for generously providing us with the Dicer fl/fl and α-CamKII-Cre mice, respectively. Finally, we thank Marie-Eve Grosjean, Hélène Obriot and Sabia Eddarkaoui (Lille, France), as well as Claudia Goupil (Quebec, Canada) and Elisabeth Larsen (Copenhagen, Denmark) for expert technical assistance.

Conflict of Interest statement. None declared.

FUNDING

This work was supported by the Fund for Scientific Research Flanders, KULeuven, Federal Office for Scientific Affairs, Belgium (IUAP P6/43/), a Methusalem grant of the KULeuven and the Flemish Government, Amytoxtau (ANR-08-MNP-002) of the French National Research Agency, Memosad (FZ-2007-200611) of the European union and an excellence grant from the Belgian 'Stichting voor Alzheimer onderzoek', the Natural Sciences and Engineering Research Council of Canada (092850), the Scottish Rite Charitable Foundation of Canada and the Lundbeck Foundation. The Wilhelm Johannsen Centre for Functional Genome Research is established by the Danish National Research Foundation.

REFERENCES

1. Ambros, V. (2004) The functions of animal microRNAs. *Nature*, **431**, 350–355.
2. Hobert, O. (2008) Gene regulation by transcription factors and microRNAs. *Science*, **319**, 1785–1786.
3. Ventura, A., Young, A.G., Winslow, M.M., Lintault, L., Meissner, A., Erkeland, S.J., Newman, J., Bronson, R.T., Crowley, D., Stone, J.R. *et al.* (2008) Targeted deletion reveals essential and overlapping functions of the miR-17 through 92 family of miRNA clusters. *Cell*, **132**, 875–886.
4. Schaefer, A., O'Carroll, D., Tan, C.L., Hillman, D., Sugimori, M., Llinas, R. and Greengard, P. (2007) Cerebellar neurodegeneration in the absence of microRNAs. *J. Exp. Med.*, **204**, 1553–1558.
5. Kim, J., Inoue, K., Ishii, J., Vanti, W.B., Voronov, S.V., Murchison, E., Hannon, G. and Abeliovich, A. (2007) A microRNA feedback circuit in midbrain dopamine neurons. *Science*, **317**, 1220–1224.
6. Davis, T.H., Cuellar, T.L., Koch, S.M., Barker, A.J., Harfe, B.D., McManus, M.T. and Ullian, E.M. (2008) Conditional loss of Dicer disrupts cellular and tissue morphogenesis in the cortex and hippocampus. *J. Neurosci.*, **28**, 4322–4330.
7. Cuellar, T.L., Davis, T.H., Nelson, P.T., Loeb, G.B., Harfe, B.D., Ullian, E. and McManus, M.T. (2008) Dicer loss in striatal neurons produces behavioral and neuroanatomical phenotypes in the absence of neurodegeneration. *Proc. Natl Acad. Sci. USA*, **105**, 5614–5619.
8. Hebert, S.S. and De Strooper, B. (2009) Alterations of the microRNA network cause neurodegenerative disease. *Trends Neurosci.*, **32**, 199–206.
9. De Pietri Tonelli, D., Pulvers, J.N., Haffner, C., Murchison, E.P., Hannon, G.J. and Huttner, W.B. (2008) miRNAs are essential for survival and differentiation of newborn neurons but not for expansion of neural progenitors during early neurogenesis in the mouse embryonic neocortex. *Development*, **135**, 3911–3921.
10. Buee, L., Bussiere, T., Buee-Scherrer, V., Delacourte, A. and Hof, P.R. (2000) Tau protein isoforms, phosphorylation and role in neurodegenerative disorders. *Brain Res. Brain Res. Rev.*, **33**, 95–130.
11. Ballatore, C., Lee, V.M. and Trojanowski, J.Q. (2007) Tau-mediated neurodegeneration in Alzheimer's disease and related disorders. *Nat. Rev. Neurosci.*, **8**, 663–672.
12. Mandelkow, E.M. and Mandelkow, E. (1998) Tau in Alzheimer's disease. *Trends Cell Biol.*, **8**, 425–427.
13. Bilen, J., Liu, N., Burnett, B.G., Pittman, R.N. and Bonini, N.M. (2006) MicroRNA pathways modulate polyglutamine-induced neurodegeneration. *Mol. Cell*, **24**, 157–163.
14. Carrettiero, D.C., Hernandez, I., Neveu, P., Papagiannakopoulos, T. and Kosik, K.S. (2009) The cochaperone BAG2 sweeps paired helical filament-insoluble tau from the microtubule. *J. Neurosci.*, **29**, 2151–2161.
15. Yu, H., Saura, C.A., Choi, S.Y., Sun, L.D., Yang, X., Handler, M., Kawarabayashi, T., Younkin, L., Fedeles, B., Wilson, M.A. *et al.* (2001) APP processing and synaptic plasticity in presenilin-1 conditional knockout mice. *Neuron*, **31**, 713–726.
16. Lind, D., Franken, S., Kappler, J., Jankowski, J. and Schilling, K. (2005) Characterization of the neuronal marker NeuN as a multiply phosphorylated antigen with discrete subcellular localization. *J. Neurosci. Res.*, **79**, 295–302.
17. Hasegawa, M., Jakes, R., Crowther, R.A., Lee, V.M., Ihara, Y. and Goedert, M. (1996) Characterization of mAb AP422, a novel phosphorylation-dependent monoclonal antibody against tau protein. *FEBS Lett.*, **384**, 25–30.
18. Planel, E., Sun, X. and Takashima, A. (2002) Role of GSK-3b in Alzheimer's disease pathology. *Drug Dev. Res.*, **56**, 491–510.
19. Iqbal, K., Alonso, A.C., Gong, C.X., Khatoon, S., Pei, J.J., Wang, J.Z. and Grundke-Iqbal, I. (1998) Mechanisms of neurofibrillary degeneration and the formation of neurofibrillary tangles. *J. Neural. Transm. Suppl.*, **53**, 169–180.
20. Churcher, I. (2006) Tau therapeutic strategies for the treatment of Alzheimer's disease. *Curr. Top. Med. Chem.*, **6**, 579–595.
21. Mazanetz, M.P. and Fischer, P.M. (2007) Untangling tau hyperphosphorylation in drug design for neurodegenerative diseases. *Nat. Rev. Drug Discov.*, **6**, 464–479.
22. McCarthy, J.J. (2008) MicroRNA-206: the skeletal muscle-specific myomiR. *Biochim. Biophys. Acta*, **1779**, 682–691.
23. Bak, M., Silahtaroglu, A., Moller, M., Christensen, M., Rath, M.F., Skryabin, B., Tommerup, N. and Kauppinen, S. (2008) MicroRNA expression in the adult mouse central nervous system. *RNA*, **14**, 432–444.
24. Mazzucchelli, C., Vantaggiato, C., Ciamei, A., Fasano, S., Pakhotin, P., Krezel, W., Welzl, H., Wolfer, D.P., Pages, G., Valverde, O. *et al.* (2002) Knockout of ERK1 MAP kinase enhances synaptic plasticity in the striatum and facilitates striatal-mediated learning and memory. *Neuron*, **34**, 807–820.
25. Peltier, H.J. and Latham, G.J. (2008) Normalization of microRNA expression levels in quantitative RT-PCR assays: identification of suitable reference RNA targets in normal and cancerous human solid tissues. *RNA*, **14**, 844–852.
26. Davoren, P.A., McNeill, R.E., Lowery, A.J., Kerin, M.J. and Miller, N. (2008) Identification of suitable endogenous control genes for microRNA gene expression analysis in human breast cancer. *BMC Mol. Biol.*, **9**, 76.
27. Hebert, S.S., Horre, K., Nicolai, L., Papadopoulou, A.S., Mandemakers, W., Silahtaroglu, A.N., Kauppinen, S., Delacourte, A. and De Strooper, B. (2008) Loss of microRNA cluster miR-29a/b-1 in sporadic Alzheimer's disease correlates with increased BACE1/beta-secretase expression. *Proc. Natl Acad. Sci. USA*, **105**, 6415–6420.
28. Nunez-Iglesias, J., Liu, C.C., Morgan, T.E., Finch, C.E. and Zhou, X.J. Joint genome-wide profiling of miRNA and mRNA expression in Alzheimer's disease cortex reveals altered miRNA regulation. *PLoS One*, **5**, e8898.
29. Cheung, E.C. and Slack, R.S. (2004) Emerging role for ERK as a key regulator of neuronal apoptosis. *Sci. STKE*, **2004**, PE45.
30. Perry, G., Roder, H., Nunomura, A., Takeda, A., Friedlich, A.L., Zhu, X., Raina, A.K., Holbrook, N., Siedlak, S.L., Harris, P.L. *et al.* (1999) Activation of neuronal extracellular receptor kinase (ERK) in Alzheimer disease links oxidative stress to abnormal phosphorylation. *Neuroreport*, **10**, 2411–2415.

31. Seger, R., Ahn, N.G., Boulton, T.G., Yancopoulos, G.D., Panayotatos, N., Radziejewska, E., Ericsson, L., Bratlien, R.L., Cobb, M.H. and Krebs, E.G. (1991) Microtubule-associated protein 2 kinases, ERK1 and ERK2, undergo autophosphorylation on both tyrosine and threonine residues: implications for their mechanism of activation. *Proc. Natl Acad. Sci. USA*, **88**, 6142–6146.
32. Ferrer, I., Blanco, R., Carmona, M., Ribera, R., Goutan, E., Puig, B., Rey, M.J., Cardozo, A., Vinals, F. and Ribalta, T. (2001) Phosphorylated map kinase (ERK1, ERK2) expression is associated with early tau deposition in neurones and glial cells, but not with increased nuclear DNA vulnerability and cell death, in Alzheimer disease, Pick's disease, progressive supranuclear palsy and corticobasal degeneration. *Brain Pathol.*, **11**, 144–158.
33. Iqbal, K., Alonso Adel, C., El-Akkad, E., Gong, C.X., Haque, N., Khatoon, S., Pei, J.J., Tsujio, I., Wang, J.Z. and Grundke-Iqbal, I. (2002) Significance and mechanism of Alzheimer neurofibrillary degeneration and therapeutic targets to inhibit this lesion. *J. Mol. Neurosci.*, **19**, 95–99.
34. Lukiw, W.J. (2007) Micro-RNA speciation in fetal, adult and Alzheimer's disease hippocampus. *Neuroreport*, **18**, 297–300.
35. Cogswell, J.P., Ward, J., Taylor, I.A., Waters, M., Shi, Y., Cannon, B., Kelnar, K., Kemppainen, J., Brown, D., Chen, C. *et al.* (2008) Identification of miRNA changes in Alzheimer's disease brain and CSF yields putative biomarkers and insights into disease pathways. *J. Alzheimers Dis.*, **14**, 27–41.
36. Wang, W.X., Rajeev, B.W., Stromberg, A.J., Ren, N., Tang, G., Huang, Q., Rigoutsos, I. and Nelson, P.T. (2008) The expression of microRNA miR-107 decreases early in Alzheimer's disease and may accelerate disease progression through regulation of beta-site amyloid precursor protein-cleaving enzyme 1. *J. Neurosci.*, **28**, 1213–1223.
37. Aubert, B., Bona, M., Boutigny, D., Couderc, F., Karyotakis, Y., Lees, J.P., Poireau, V., Tisserand, V., Zghiche, A., Grauges, E. *et al.* (2008) Exclusive branching-fraction measurements of semileptonic tau decays into three charged hadrons, into phipi(-)nu tau, and into phi K(-)nu tau. *Phys. Rev. Lett.*, **100**, 011801.
38. Niwa, R., Zhou, F., Li, C. and Slack, F.J. (2008) The expression of the Alzheimer's amyloid precursor protein-like gene is regulated by developmental timing microRNAs and their targets in *Caenorhabditis elegans*. *Dev. Biol.*, **315**, 418–425.
39. Hebert, S.S., Horre, K., Nicolai, L., Bergmans, B., Papadopoulou, A.S., Delacourte, A. and De Strooper, B. (2009) MicroRNA regulation of Alzheimer's amyloid precursor protein expression. *Neurobiol. Dis.*, **33**, 422–428.
40. Hebert, S.S. and De Strooper, B. (2007) Molecular biology. miRNAs in neurodegeneration. *Science*, **317**, 1179–1180.
41. Eacker, S.M., Dawson, T.M. and Dawson, V.L. (2009) Understanding microRNAs in neurodegeneration. *Nat. Rev. Neurosci.*, **10**, 837–841.
42. Bushati, N. and Cohen, S.M. (2008) MicroRNAs in neurodegeneration. *Curr. Opin Neurobiol.*, **18**, 292–296.
43. Galas, M.C., Dourlen, P., Begard, S., Ando, K., Blum, D., Hamdane, M. and Buee, L. (2006) The peptidylprolyl *cis*/*trans*-isomerase Pin1 modulates stress-induced dephosphorylation of tau in neurons. Implication in a pathological mechanism related to Alzheimer disease. *J. Biol. Chem.*, **281**, 19296–19304.
44. Harfe, B.D., McManus, M.T., Mansfield, J.H., Hornstein, E. and Tabin, C.J. (2005) The RNaseIII enzyme Dicer is required for morphogenesis but not patterning of the vertebrate limb. *Proc. Natl Acad. Sci. USA*, **102**, 10898–10903.
45. Hebert, S.S., Serneels, L., Tolia, A., Craessaerts, K., Derks, C., Filippov, M.A., Muller, U. and De Strooper, B. (2006) Regulated intramembrane proteolysis of amyloid precursor protein and regulation of expression of putative target genes. *EMBO Rep.*, **7**, 739–745.
46. Bretteville, A., Ando, K., Ghestem, A., Loyens, A., Begard, S., Beauvillain, J.C., Sergeant, N., Hamdane, M. and Buee, L. (2009) Two-dimensional electrophoresis of tau mutants reveals specific phosphorylation pattern likely linked to early tau conformational changes. *PLoS One*, **4**, e4843.
47. Schindowski, K., Bretteville, A., Leroy, K., Begard, S., Brion, J.P., Hamdane, M. and Buee, L. (2006) Alzheimer's disease-like tau neuropathology leads to memory deficits and loss of functional synapses in a novel mutated tau transgenic mouse without any motor deficits. *Am. J. Pathol.*, **169**, 599–616.
48. Planel, E., Miyasaka, T., Launey, T., Chui, D.H., Tanemura, K., Sato, S., Murayama, O., Ishiguro, K., Tatebayashi, Y. and Takashima, A. (2004) Alterations in glucose metabolism induce hypothermia leading to tau hyperphosphorylation through differential inhibition of kinase and phosphatase activities: implications for Alzheimer's disease. *J. Neurosci.*, **24**, 2401–2411.